MITSUBISHI ELECTRIC RESEARCH LABORATORIES
http://www.merl.com

Experimental Throughput Analysis in Screen-Camera Visual MIMO Communications

Fujihashi, T.; Koike-Akino, T.; Watanabe, T.; Orlik, P.V.

TR2016-169 December 2016

Abstract

Screen-camera communication, which uses a liquid crystal display (LCD) screen and camera image sensors, has been an attractive variant of visible light communications (VLC) since display and camera have been equipped with in various mobile devices. To improve transmission rates, we investigate the impact of nonlinear channel equalization and nonbinary channel coding as well as high-order modulation schemes. Equalization techniques can reduce the effect of channel impairments, such as color mixing. Nonbinary coding improves reliability of highorder modulation and thus increases the transmission rate. Experimental evaluations using an LCD screen and camera demonstrate that our proposed scheme achieves 3.6- 2.4 times higher transmission rates compared to existing schemes for a communication distance of 40- 100 cm.

IEEE Global Communications Conference (GLOBECOM)

Experimental Throughput Analysis in Screen-Camera Visual MIMO Communications

Takuya Fujihashi†*, Toshiaki Koike-Akino†, Philip V. Orlik†, and Takashi Watanabe*
†Mitsubishi Electric Research Laboratories (MERL), Cambridge, MA 02139, USA
*Graduate School of Information and Science, Osaka University, Osaka, Japan

***Abstract*—Screen-camera communication, which uses a liquid crystal display (LCD) screen and camera image sensors, has been an attractive variant of visible light communications (VLC) since display and camera have been equipped with in various mobile devices. To improve transmission rates, we investigate the impact of nonlinear channel equalization and nonbinary channel coding as well as high-order modulation schemes. Equalization techniques can reduce the effect of channel impairments, such as color mixing. Nonbinary coding improves reliability of high-order modulation and thus increases the transmission rate. Experimental evaluations using an LCD screen and camera demonstrate that our proposed scheme achieves 3.6–2.4 times higher transmission rates compared to existing schemes for a communication distance of 40–100 cm.**

I. Introduction

Visible light communication (VLC) has emerged as a promising alternative/complementary technology to conventional radio-frequency (RF) wireless communications. VLC is expected to lead to many wireless applications, such as inter/intra vehicle communications [1], near field communication [2], [3], and indoor localization [4].

Screen-camera communication [5], [6] is one kind of VLC technologies, where a screen and a camera can transmit information using images on the screen. For screen-camera communications, digital bits are encoded in the screen image on devices, e.g., laptop computers and smart phones. A receiver equipped with camera image sensors captures the screen to decode the information. The use of screen and camera can form so-called multi-input multi-output (MIMO) systems in which optical transmissions by an array of light emitting devices are received by an array of photo-diode elements. Although high-definition screen and camera can realize massive spatial multiplexing gain to transfer a large amount of information bits at once, frame rates of those screen and camera are severely constrained in general (typically tens of frames per second).

A major challenge of the screen-camera communications is to increase the transmission rate in nonlinear channels with ambient noise. In particular, there are three issues in such links as follows. First, an encoded image on the screen is distorted due to receiver's perspective. When the receiver captures the encoded image on a rectangular screen from a certain angle, the captured image will become a trapezoid. This phenomenon is referred to as perspective distortion [7]. Second, the luminance of encoded image is impaired by ambient lights. This impairment causes errors in the encoded information, and resulting in a low transmission rate. Third, the spectrum sensitivity of red, green, and blue channels on the camera sensor is not orthogonal. In other words, the output of one color channel may be degraded by the intensity of other color channels. This is known as a color mixing.

To overcome the above-mentioned issues, some approaches [8]–[12] have been proposed for screen-camera links to improve the transmission rates. For example, PixNet [8] uses orthogonal discrete multi-tone (DMT) for single-color channel transmission. In PixNet, the effect of perspective distortion and ambient lights can be also reduced. Another approach in [9] discusses the effect of high-order modulation for the communication with single color channel. In addition, some approaches [10], [12] use three color channels, i.e., red, green, and blue, to improve the transmission rate. However, the increase of transmission rates are still marginal.

To increase the transmission rate in screen-camera communications, we investigate linear and nonlinear channel equalizations [13]–[15]. Although how to design linear channel equalization in VLC was discussed in [16], there was no comparative evaluation of the throughput improvement in screen-camera communications. In addition, we analyze both binary and nonbinary coding systems [17], [18]. For wireless [19] and optical communications [20], nonbinary codes have been used to improve the reliability of communications using multilevel modulation formats. To accomplish high transmission rate in screen-camera communications, we introduce the nonbinary coding together with high-order modulation.

Accordingly, we propose a new screen-camera communication scheme, which integrates three color channels, high-order modulation, nonbinary coding, and nonlinear channel equalization. Specifically, a sender uses multilevel quadrature-amplitude modulation (QAM) and assigns the modulated data to red, green, and blue color channels. For the multilevel modulated data, our scheme uses nonbinary coding to achieve high reliability. At the receiver side, the decoder carries out linear/nonlinear channel equalization in frequency domain to mitigate impairments in screen-camera channels. Experimental evaluations using a screen and camera sensor show that the proposed scheme increases the transmission rates, up to 3.6 times higher than existing studies.

T. Fujihashi conducted this research while he was an intern at MERL.

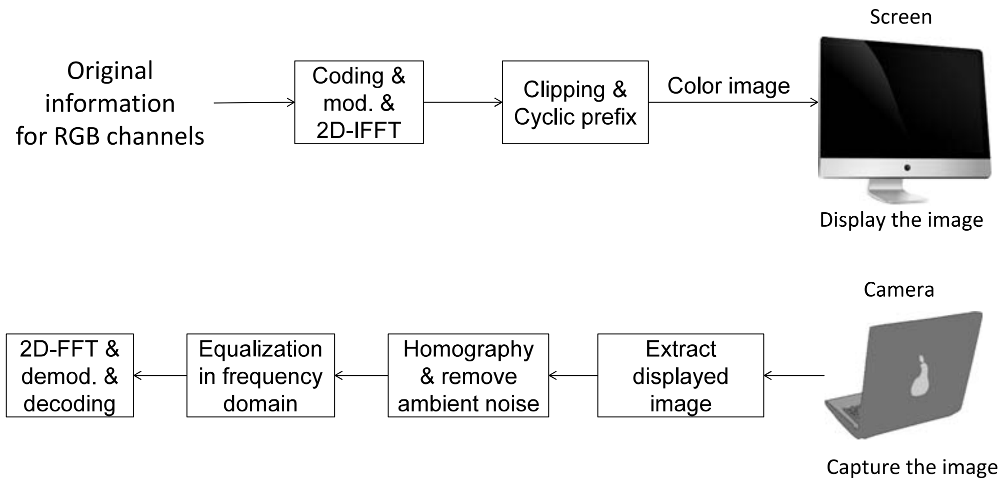

Fig. 1. Sender and receiver operation in screen-camera visual MIMO communications.

II. Screen-Camera Visual MIMO Communications

A. Overview

The purpose of our study is to achieve higher transmission rate in screen-camera communications. Fig. 1 shows the schematic of our proposed scheme. We use a pair of screen and camera as the sender and receiver, respectively. Note that there are three major differences from RF wireless communications. First, input values for the screen, i.e., pixel luminance values, should not be complex-valued numbers. Second, the input values are two dimensional (2D) in spatial domain. Third, the pixel luminance values typically range over finite non-negative integers, i.e., $0, 1, \ldots, 255$ for 8-bit quantization.

Based on the constraints, the sender first encodes original information with nonbinary coding, followed by 2^M-ary QAM modulation, and arranges the modulated symbols into a 2D matrix. The modulated coefficients are then transformed to pixel luminance values by taking inverse 2D fast Fourier transform (FFT) operation, and clipped according to the luminance range. Finally, cyclic prefix is added to the two dimensional values prior to display. At the receiver side, pixel luminance values are captured by camera sensors and then extracts the transmitted region from the captured values using a edge detection algorithm. We then mitigate the effect of perspective distortion and ambient lights. Finally, the filtered pixel values are equalized, transformed to frequency representation by 2D-FFT, and decoded to obtain original information.

B. Sender

1) Basis Transform for Precoding: In order to be robust against inter-pixel interference, we use a precoding technique based on 2D-FFT. The stream of QAM-modulated symbols are transformed to pixel luminance values using inverse 2D-FFT for each color channel. As mentioned above, the screen only accepts real values as the input luminance. To ensure output values from inverse 2D-FFT are purely real, we arrange the 2D matrix to be Hermitian symmetry. Note that the output from inverse FFT will be entirely real when the input values are Hermitian.

More specifically, we suppose the use of screen image having a resolution of $H \times W$ pixels for each color channel, for transmitting $3HW$ real values in total over three color channels. For each color channel, modulated QAM symbols are arranged into a matrix of size $H \times (W/2)$ and the 1D inverse FFT is carried out for each column. The FFT coefficients are organized to be Hermitian symmetry by assigning the complex conjugate of the value at the (i, j)-th pixel to the $(i, -j)$-th pixel. The coefficients in each row are then fed into inverse FFT. The resulting HW values are all real and can be sent as screen image.

As an alternative basis function, we also investigate discrete cosine transform (DCT), which may be suited for real-valued data transform.

2) Clipping: We consider 8 bits for quantization representation of pixel luminance for screen images. To ensure the output of FFT being within the rage between 0 and 255, the pixel luminance values are shifted and scaled to have a mean of $255/2$ and a variance of $(255/2c_{\mathrm{tail}})^2$, where c_{tail} is a clipping parameter. All values outside the range between 0 and 255 are clipped to 0 and 255, respectively. When the FFT size is large enough, the luminance values may follow a Gaussian distribution according to the central limit theorem. By adjusting the clipping parameter c_{tail}, we can control the probability of clipping events. For example, 99.99% of luminance values before clipping may lie within the 8-bit integer range for $c_{\mathrm{tail}} = 4$.

3) Cyclic Prefix: In screen-camera links, since light emitted from an LCD screen is diffusive in nature, each photo detector of camera sensors receives multiple lights from nearby LCD pixels. As a result, the LCD pixels are blended into one camera pixel in particular for long distance and mobile devices due to blur. The FFT-based transmission is insensitive to linear inter-pixel interference induced by the blur. However, this

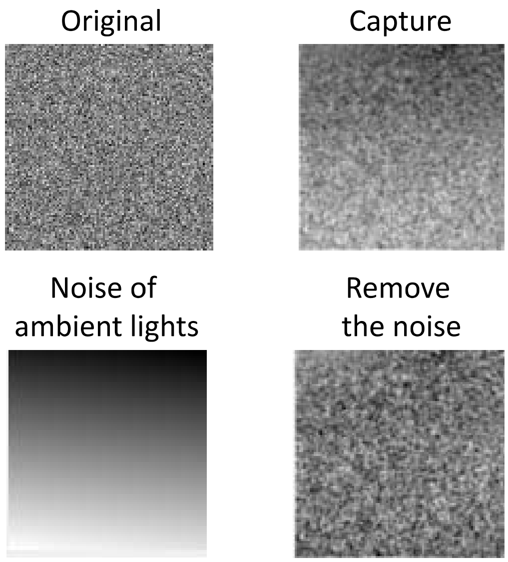

Fig. 2. An example of ambient light correction. A captured image is distorted due to ambient lights. Our scheme calculates the ambient noise by using a least-squares fitting function and then subtracts the noise from the captured image.

blending effect can still cause performance degradation at edges of the screen images, i.e., background values outside the encoded pixels can interfere. To mitigate the edge effect, pixels with white color are appended around the encoded values as cyclic prefix. Finally, the encoded values with cyclic prefix are displayed on the screen with black background. Note that the white cycle prefix is also useful for edge detection at the receiver.

C. Receiver

1) Data Extraction: Receiver's camera first captures an image, which contains the transmitter's screen, for communications. Prior to decoding, the area of encoded pixels is extracted from the captured image. This requires the receiver to detect the four corners of the area. In our implementation, the encoded values can be extracted by detecting edges between white cyclic prefix and black background.

2) Perspective and Ambient Light Correction: The extracted image is typically trapezoid and shifted pixel luminance, i.e., perspective distortion and ambient light distortion. We correct the perspective distortion by using homography operation [21]. Specifically, a trapezoid image can be transformed to a rectangle image based on four corners of images.

The proposed scheme then reduces the noise of ambient lights from the rectangle image. We recall the mean of encoded pixel values is shifted to $255/2$ at the transmitter, and thus shall align the mean of pixel luminance values of the rectangle image to zero before demodulation. To this end, our scheme subtracts the pixel values by the output of a best-fit linear function of $f(i,j) = ai + bj + c$ by means of least-squares method, where i and j are vertical index and horizontal index for pixels, respectively.

Fig. 2 shows an example of ambient light correction. As shown in the captured image, the upper luminance is darker than the lower luminance due to the ambient lights. Based on the output of a fitting function, the receiver estimates the noise from ambient lights and then subtracts the noise from the captured image to reduce impairments.

3) Decoding: The filtered luminance values are then fed into 2D-FFT and equalized to mitigate impairments due to screen-camera channels. After the receiver uses standard 2^M-ary QAM demodulation to calculate log-likelihood ratio (LLR), the channel decoding is carried out for the LLR values to obtain original information.

D. Linear/Nonlinear Equalization

In screen-camera communications, transmitted symbols are impaired by channel gains and an effective noise in frequency domain, e.g., due to motion blur. Let $\mathbf{y}_{i',j'}$ denote a 3×1 vector of received symbols at (i', j')-th frequency component. Each row represents received symbols from red, green, and blue color channels, respectively. We assume that the received symbols in screen-camera links are modeled as nonlinear systems as follows:

$$\mathbf{y}_{i',j'} = \mathbf{H}_{i',j'} \phi(\mathbf{x}_{i',j'}) + \mathbf{z}_{i',j'}, \tag{1}$$

where $\mathbf{x}_{i',j'}$ is a 3×1 vector of transmitted symbols in frequency domain, $\mathbf{H}_{i',j'}$ is a $3 \times K$ channel gain matrix, $\mathbf{z}_{i',j'}$ is a 3×1 additive white Gaussian noise (AWGN) vector with a noise variance of $\sigma^2_{i',j'}$. Here, $\phi(\cdot)$ denotes a nonlinear kernel expansion and K is an expansion cardinality. For example, the second-order Volterra series expansion (including an offset term) [13]–[15] is expressed as $\phi(\mathbf{x}) = [1, \mathbf{x}^{\mathrm{T}}, \mathbf{x}^{\mathrm{T}} \otimes \mathbf{x}^{\mathrm{T}}]^{\mathrm{T}}$ with $K = 1 + 3 + 3^2 = 13$. Here, $\otimes$ represents Kronecker product and $[\cdot]^{\mathrm{T}}$ is a transpose.

Rather than using maximum-likelihood equalization for $\phi(\mathbf{x}_{i',j'})$ with expanded channel estimation, we employ minimum mean-square error (MMSE) equalization for the Volterra series expansion of the received symbols, i.e., $\phi(\mathbf{y}_{i',j'})$. Specifically, MMSE filter weights of size $3 \times K$ are obtained as follows:

$$\mathbf{G}_{i',j'} = \mathbb{E}\big[\mathbf{x}_{i',j'} \phi(\mathbf{y}_{i',j'})^{\dagger}\big] \mathbb{E}\big[\phi(\mathbf{y}_{i',j'}) \phi(\mathbf{y}_{i',j'})^{\dagger}\big]^{-1}, \tag{2}$$

where $\mathbb{E}[\cdot]$ and $[\cdot]^{\dagger}$ denote the expectation and Hermitian transpose, respectively. In practice, the expectation is taken place by averaging multiple measurements in the past. In this paper, we consider either first-order or second-order Volterra series expansion for $\phi(\cdot)$, respectively, as linear equalizer (LE) or nonlinear equalizer (NLE). Finally, the received symbols are equalized using the MMSE filter as follows:

$$\hat{\mathbf{x}}_{i',j'} = \mathbf{G}_{i',j'} \phi(\mathbf{y}_{i',j'}). \tag{3}$$

E. Nonbinary Channel Coding

To further improve the transmission rate, we use nonbinary channel coding based on low-density parity-check (LDPC) codes over Galois field of $\mathbb{GF}(Q)$ [18] for 2^M-ary QAM transmissions. For the Galois field size of $Q = 2^M$, a sender

Fig. 3. Experimental equipment.

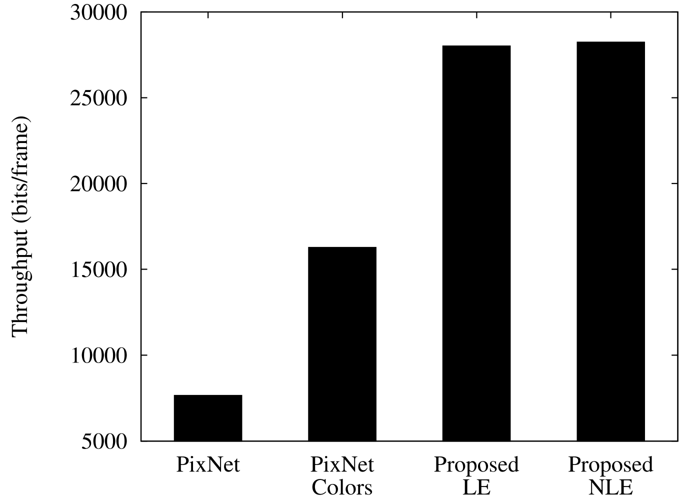

Fig. 4. Throughput performance with 4-QAM modulation at 40 cm distance: PixNet uses binary LDPC codes, while the proposed scheme uses nonbinary LDPC codes.

encodes every M-bit tuple of original data by using the Q-ary LDPC code. The encoded bits are sequentially mapped to symbol constellations with 2^M-ary modulation schemes. At the receiver side, the received symbols are demodulated to calculate an LLR vector $[L_0, L_1, \ldots, L_{Q-1}]$. The q-th LLR value is expressed as follows:

$$L_q = \ln \frac{\Pr(\hat{x}|b=0)}{\Pr(\hat{x}|b=q)}, \tag{4}$$

where $\Pr(\hat{x}|b = q) \propto \exp\bigl(-\frac{1}{\sigma^2}|\hat{x} - \chi_q|^2\bigr)$ denotes the likelihood, i.e., the probability that the equalized signal is $\hat{x}$ when the transmitted symbol is χ_q, which is the q-th QAM constellation. The LLR vector is fed into a nonbinary LDPC decoder based on FFT Q-ary sum-product algorithm (QSPA).

III. Performance Evaluations

A. Experimental Methodology

We use view sonic VG2228wm with a resolution of 1920×1080 and MacBook Pro 13-inch with 720p camera as a display screen and camera, respectively, as shown in Fig. 3. To display encoded values on the screen, we use Psychophysics Toolbox Version 3 [22], which is a free set of Matlab functions with a precise control of display timing.

We evaluate the achievable throughput of screen-camera communication schemes in terms of bits per one received frame. The throughput is defined as follows.

$$R = B \cdot \mathcal{I}(X;Y), \tag{5}$$

where R denotes throughput (bits/frame), B is the total number of transmitted bits in one encoded image, and $\mathcal{I}(X;Y)$ is mutual information between a transmitted image X and received image Y. Here, the mutual information for nonbinary coding is calculated from the LLR vector as follows:

$$\mathcal{I}(X;Y) = 1 - \mathbb{E}\left[\log_Q \left(\sum_{q=0}^{Q-1} \exp(-L_q)\right) \middle| b = 0\right]. \tag{6}$$

When binary coding is considered, the mutual information is obtained analogously with $Q = 2$.

Unless otherwise stated, we evaluate the achievable throughput at a distance between the screen and camera of 40 cm. We also make an analysis of the throughput for different distances of 60, 80, and 100 cm. We use 90 images with a resolution of $H \times W = 100 \times 100$ for communications. For each image, we set a clipping parameter of c_{tail} to 4. Each image is displayed at the center position of the LCD screen.

B. Baseline Performance

In Fig. 4, we show the baseline performance of screen-camera links for four reference schemes: PixNet [8], PixNet with color channels, proposed scheme with linear equalization, and proposed scheme with nonlinear equalization. All the reference schemes use 4-QAM for the modulation format. PixNet uses the binary LDPC code for channel coding, and encoded values are displayed on green color channel for simplicity. The other schemes use red, green, and blue color channels. The proposed schemes use the nonbinary LDPC code for channel coding.

From Fig. 4, we can observe the following two points:

- The proposed scheme with NLE achieves the highest throughput.
- Even without NLE, our scheme realizes higher performance compared to the existing PixNet schemes because color mixing can be mitigated by LE.

For example, the throughput of our scheme with NLE is 3.6 times higher than PixNet and 1.7 times higher than PixNet with color channels. It suggests that equalization techniques are more advantageous for high-speed screen-camera communications.

C. Throughput vs. Distance

Previous evaluations considered a fixed communication distance of 40 cm. However, when we use mobile devices for the communications, the distance between a sender and receiver

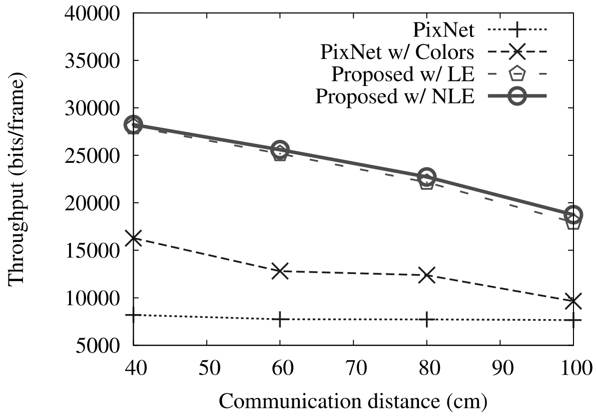

Fig. 5. Throughput with different communication distances.

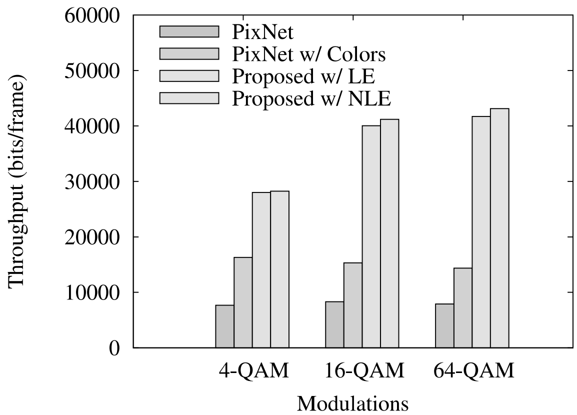

Fig. 6. Throughput with different order of modulations at a distance of 40 cm.

may vary. To evaluate the impact of the distance in throughput, we compare the achievable throughput at a distance of 60, 80, or 100 cm in addition to 40 cm.

Fig. 5 shows the throughput as a function of communication distance. Even in a longer distance, the proposed scheme keeps a higher throughput compared to the conventional schemes. For instance, the proposed scheme achieves 2.4 times higher throughput than PixNet and 1.9 times higher throughput than PixNet with color channels at a communication distance of 100 cm. It is also seen that PixNet without color channels is more robust than PixNet with color channels. It indicates that color mixing can be dominant in long-range communications.

D. Impact of High-Order Modulation

To increase the throughput, we shall use higher-order modulation schemes than 4-QAM. In Fig. 6, we show the effect of high-order modulation schemes on throughput performance with 4-QAM, 16-QAM, and 64-QAM at a communication distance of 40 cm. From Fig. 6, we can see the following results:

- High-order modulation boosts the performance improvement in the proposed schemes.

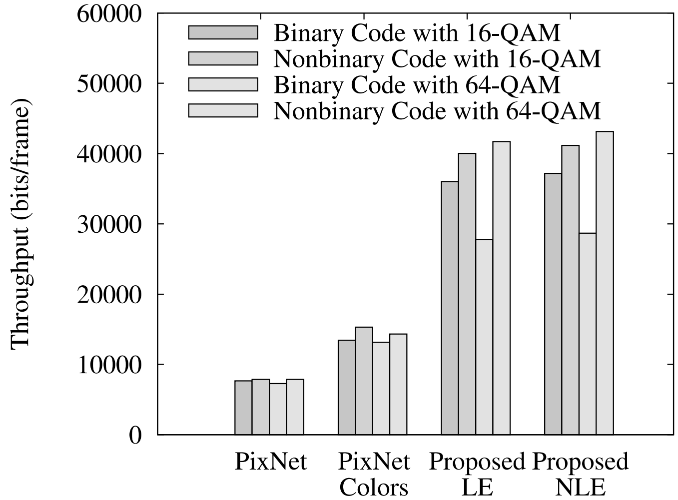

Fig. 7. Throughput with binary and nonbinary codes.

- In the existing schemes, high-order modulation schemes does not always improve the throughput because demodulation can fail without equalization.

For example, the proposed scheme with 64-QAM offers 1.5 times higher throughput compared to the 4-QAM scheme. From these results, it is verified that high-order modulation schemes in conjunction with equalization techniques are effective for achieving high throughput in screen-camera communications.

It is also observed that the nonlinear equalization can be more effective for higher-order modulation schemes although the performance improvement is still marginal. We leave the study of designing more effective nonlinear kernels as a future work.

E. Impact of Nonbinary Coding

This section discusses the contributions of nonbinary coding for performance improvement. In Fig. 7, we compare the throughput with binary and nonbinary codes, for 16-QAM and 64-QAM. It is demonstrated that the nonbinary coding offers performance improvement in particular for higher-order modulation with equalizations in our proposed scheme. From this figure, it is strongly recommended to integrate high-order modulation, nonbinary coding, and equalization for increasing the achievable throughput.

F. Impact of Basis Functions

Our proposed scheme (as well as PixNet) uses FFT-based precoding for transforming original information onto screen images. We now evaluate the impact of different basis transforms, i.e., no precoding and DCT, as an alternative of FFT. Note that imaginary parts of $H \times (W/2)$ QAM-modulated symbols are mapped to the rest of pixels to be real-valued images for DCT and no precoding cases. While the modulated values are directly mapped to pixels at an LCD screen for the case without precoding, an inverse 2D-DCT is taken

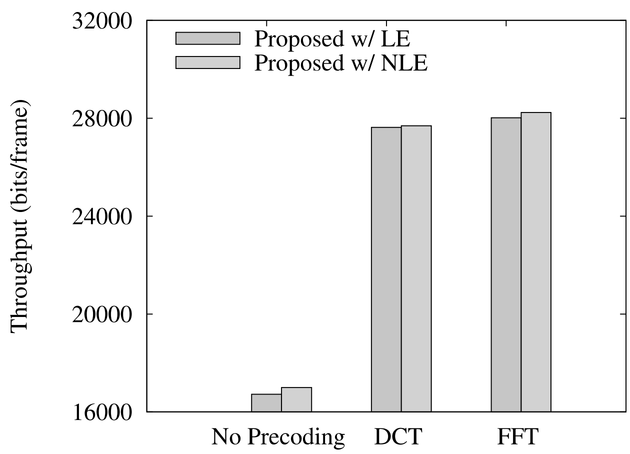

Fig. 8. Throughput with different precoding techniques.

place before displaying the pixel images for the case of DCT precoding.

In Fig. 8, we compare the throughput with different precoding methods. From this figure, it is seen that higher throughput can be achieved by precoding, i.e., either DCT or FFT. For example, the throughput of FFT-based scheme is 1.7 times higher than no precoding scheme. For no precoding scheme, modulated values are severely impaired by inter-pixel interference even after linear and nonlinear equalizations. The proposed scheme with FFT-based precoding achieves slightly better performance than DCT-based precoding.

IV. Conclusion

This paper proposed a new screen-camera communication scheme to improve the throughput of the visual MIMO links. To realize the improvement, our proposed scheme integrates color channels, high-order modulation, linear/nonlinear channel equalization, and nonbinary coding. We experimentally evaluated the achievable throughput of screen-camera communications, using a consumer-grade LCD screen and camera. Through the experiments, we demonstrated that the proposed scheme achieves 3.6 times higher throughput than conventional schemes. We also demonstrated that our scheme keeps higher throughput than the existing schemes for longer communication distance between the screen and camera. To the best of our knowledge, this is the first experimental demonstration exploiting linear/nonlinear channel equalization and nonbinary coding for screen-camera communications in the literature.

Acknowledgment

This work was partly supported by JSPS KAKENHI Grant Number 14J09461.

References

[1] T. Yamazato, I. Takai, H. Okasa, T. Fujii, T. Yendo, S. Arai, M. Andoh, T. Harada, K. Yasutomi, K. Kagawa, and S. Kawahito, "Image-sensor-based visible light communication for automotive applications," *IEEE Communication Magazine*, vol. 52, no. 7, pp. 88–97, 2014.

[2] A. Wang, S. Ma, C. Hu, J. Huai, C. Peng, and G. Shen, "Enhancing reliability to boost the throughput over screen-camera links," in *ACM Annual International Conference on Mobile Computing and Networking*, 2014, pp. 41–52.

[3] W. Hu, H. Gu, and Q. Pu, "Lightsync: Unsynchronized visual communication over screen-camera links," in *ACM Annual International Conference on Mobile Computing and Networking*, 2013, pp. 15–26.

[4] Y.-S. Kuo, P. Pannuto, K.-J. Hsiao, and P. Dutta, "Luxapose: indoor positioning with mobile phones and visible light," in *ACM Annual International Conference on Mobile Computing and Networking*, 2014, pp. 447–458.

[5] P. H. Pathak, X. Feng, P. Hu, and P. Mohapatra, "Visible light communication, networking and sensing: A survey, potential and challenges," *IEEE Communications Surveys & Tutorials*, vol. 17, no. 4, pp. 2047–2077, 2015.

[6] R. LiKamWa, D. Ramirez, and J. Holloway, "Styrofoam: A tightly packed coding scheme for camera-based visible light communication," in *ACM MobiCom workshop on Visible light communication systems*, 2014, pp. 27–32.

[7] A. Ashok, S. Jain, M. Gruteser, N. Mandayam, W. Yuan, and K. Dana, "Capacity of pervasive camera based communication under perspective distortions," in *IEEE International Conference on Pervasive Computing and Communications*, 2014, pp. 114–120.

[8] S. Perli, N. Ahmad, and D. Katabi, "Pixnet: Interference-free wireless links using LCD-camera pairs," in *ACM Annual International Conference on Mobile Computing and Networking*, 2010, pp. 137–148.

[9] W. Huang, C. Gong, P. Tian, and Z. Xu, "Experimental demonstration of high-order modulation for optical camera communication," in *IEEE Symposium on Signal Processing for Optical Wireless Communications*, 2015, pp. 1027–1031.

[10] T. Hao, R. Zhou, and G. Xing, "COBRA: Color barcode streaming for smartphone systems," in *ACM International Conference on Mobile Systems, Applications, and Services*, 2012, pp. 85–98.

[11] W. Hu, J. Mao, Z. Huang, Y. Xue, J. She, K. Bian, and G. Shen, "Strata: Layered coding for scalable visual communication," in *ACM Annual International Conference on Mobile Computing and Networking*, 2014, pp. 79–90.

[12] W. Du, J. C. Liando, and M. Li, "SoftLight: Adaptive visible light communication over screen-camera links," in *IEEE Annual conference on Computer Communications*, 2016, pp. 1–9.

[13] M. Schetzen, *The Volterra and Wiener Theories of Nonlinear Systems*. Kriger, 1989.

[14] N. Mallouki, B. Nsiri, S. Mhatli, M. Ghanbarisabagah, W. Hakimi, M. Ammar, and E. Giacoumidis, "Analysis of full Volterra nonlinear equalizer for downlink LTE system," in *Wireless Telecommunications Symposium*, 2015, pp. 1–6.

[15] G. B. Giannakis and E. Serpedin, "Linear multichannel blind equalizers of nonlinear FIR Volterra channels," *IEEE Transactions on Signal Processing*, vol. 45, no. 1, pp. 67–81, 1997.

[16] S. Hranilovic and F. R. Kschischang, "A pixelated mimo wireless optical communication system," *IEEE Journal of Selected Topics in Quantum Electronics*, vol. 12, no. 4, pp. 859–874, 2006.

[17] U. Wachsmann, R. F. H. Fischer, and J. B. Huber, "Multilevel codes: Theoretical concepts and practical design rules," *IEEE Transactions on Information Theory*, vol. 45, no. 5, pp. 1361–1391, 1999.

[18] D. Declercq and M. Fossorier, "Decoding algorithms for nonbinary LDPC codes over GF," *IEEE Transactions on Communications*, vol. 55, no. 4, pp. 633–643, 2007.

[19] S. Pfletschinger, A. Mourad, E. Lopez, D. Declercq, and G. Bacci, "Performance evaluation of non-binary LDPC codes on wireless channels," in *ICT Mobile and Wireless Communications Summit*, 2009.

[20] I. B. Djordjevic and B. Vasic, "Nonbinary LDPC codes for optical communication systems," *IEEE Photonics Technology Letters*, vol. 17, no. 10, pp. 2224–2226, 2005.

[21] E. Vincent and R. Laganiere, "Detecting planar homographies in an image pair," in *International Symposium on Image and Signal Processing and Analysis*, 2001, pp. 1–6.

[22] D. H. Brainard, "The psychophysics toolbox," in *Spatial Vision 10*, 2016, pp. 433–436.